Journal of Structural Geology, Vol. 14, No. 2, pp. 215 to 223, 1992
Printed in Great Britain

0191-8141/92 $05.00 + 0.00
© 1992 Pergamon Press plc

Estimation of the potential type of faulting in relation to the stress field: the North Aegean case study

E. D. CHIOTIS

Institute of Geology and Mineral Exploration, 70 Messogion Avenue, 115 27 Athens, Greece

and

C. E. TSOUTRELIS

Mining Engineering Department, National Technical University, 42 Patission Street, 106 82 Athens, Greece

(*Received* 7 *December* 1989; *accepted in revised form* 2 *July* 1991)

Abstract—The relation between the angle of slip during fault reactivation and the applied stress field is investigated through a plot of the deviatoric stress ratio $r = (\sigma_v - \sigma_h)/(\sigma_H - \sigma_h)$ vs the fault strike direction measured from σ_H, assuming that one of the principal stresses, σ_v, is vertical. This approach is applied to the North Aegean trough fault zone on the basis of neotectonic data presented previously by other authors, and conclusions are drawn as to the potential type of faulting along the trough since late Miocene. The same reasoning is also applied to earthquake focal mechanisms of the Northern Aegean region.

INTRODUCTION

THE initiation of faults in idealized continuous rock masses can be interpreted on the basis of the Coulomb theory of shear failure and the type of faulting can be classified according to the relative magnitude of the principal stresses (Anderson 1951). According to the Andersonian theory, in a homogeneous rock, fracture takes place on one or both of a pair of conjugate planes which pass through the direction of the intermediate principal stress, σ_2, and are equally inclined at angles of $<45°$ to the direction of the greatest principal stress, σ_1. Compressive stresses are taken positive in this work and therefore $\sigma_1 \geq \sigma_2 \geq \sigma_3$. The principal stresses can alternatively be designated in terms of their orientation, assuming that one of them is vertical, with σ_v, σ_H and σ_h corresponding to the vertical, greatest horizontal and least horizontal principal stress, respectively. Thrust faulting is expected where $\sigma_3 = \sigma_v$, strike-slip faulting where $\sigma_2 = \sigma_v$, and normal faulting where $\sigma_1 = \sigma_v$.

In nature, however, failure by activation of pre-existing faults may be easier than the formation of new faults. In cases of fault reactivation the Coulomb criterion of failure is modified, considering sliding resistance along pre-existing fractures instead of fracturing. As shown by Bott (1959), for fixed directions of principal stresses, the angle of sliding depends on both the orientation of the pre-existing fault plane and the relative magnitudes of the principal stresses. Conversely, the determination of both the directions of the principal axes of stress and the deviatoric stress ratio, on the basis of the striations on a population of fractures reactivated during a single tectonic event, relies on the assumption that faulting results from the sliding along pre-existing faults (e.g. Arthaud 1969, Carey 1976). Furthermore, Arthaud points out that two sets of faults approaching Anderson's model may occur in nature, but, in general, fault directions are more dispersed.

In addition to the concept of fault reactivation another important aspect concerns the possible directions of pre-existing faults. Brace & Kohlstedt (1980) estimated the frictional strength of the lithosphere assuming that fractures of all orientations exist. Similarly Reches (1983) assumes that prior to deformation many discontinuity surfaces with random orientation exist and that the applied deformation is accommodated by slip along only a few sets of preferred faults, selected to minimize the dissipation of energy under a given strain. In this paper a slightly different approach is followed. It is postulated that the important pre-existing faults of the continental crust in a broader region are arranged along distinct fault zones, and that both regional deformation and seismicity are accommodated mainly by slip along them over significant periods of time. The North Aegean trough is treated here as such a fault zone. Obviously the above principle is scale sensitive and applies to the higher structural scale in Arthaud's sense. However, other models like Anderson's and Reches' may be applicable at lower scales.

Sibson (1985) considered the conditions for reactivation of existing faults in the simplest case where the normal to the fault plane lies in the σ_1–σ_3 plane. In this particular case the frictional failure criterion is simplified to the equation:

$$\sigma_1'/\sigma_3' = (1 + \mu\cot\theta)/(1 - \mu\tan\theta), \qquad (1)$$

where σ_1' and σ_3' are the greatest and least effective principal compressive stresses, respectively, μ is the static coefficient of friction and θ the angle of the fault plane to σ_1.

Philip (1987) distinguished four types of tectonic deformation based on the deviatoric stress ratio:

$$R = \frac{\sigma_2 - \sigma_3}{\sigma_1 - \sigma_3}. \quad (2)$$

These may involve a combination of different types of faults as follows:

(1) combination of strike-slip and reverse faults, whereby the vertical principal stress, σ_v, is either σ_2 or σ_3, σ_2 tends to σ_3 and R tends to zero;

(2) combination of strike-slip and normal faults with the vertical principal stress, σ_v, being σ_2 or σ_1; R tends to 1 and σ_2 to σ_1;

(3) constrictive deformation of thrust faulting, where $\sigma_v = \sigma_3$, σ_2 comes close to σ_1, R tends to 1 and $\sigma_2 \gg (\sigma_1 + \sigma_3)/2$;

(4) radial extension with $\sigma_v = \sigma_1$, σ_3 tending to σ_2, R to 0 and $(\sigma_1 + \sigma_3)/2 \gg \sigma_2$.

FAULTING TYPE DIAGRAM

Reactivation of pre-existing faults can be studied on the basis of Bott's equation (1959):

$$\tan \omega = \frac{n}{lm}\left[m^2 - (1 - n^2)\frac{\sigma_z - \sigma_x}{\sigma_y - \sigma_x}\right], \quad (3)$$

where σ_x, σ_y, σ_z are the principal stresses in the crust, σ_z is assumed vertical, l, m, n are the direction cosines of the normal to the fault plane, relative to the principal stress axes, and ω is the angle of sliding measured from the strike direction of the fault. It follows from equation (3) that the angle of sliding, and therefore the type of faulting, is entirely determined from the orientation of the fault and the deviatoric stress ratio. Equation (3) also provides the possible directions of sliding in the case of fault reactivation. However, whether reactivation takes place or not for a given state of stress depends on three other factors: sliding friction along the fault, pore pressure and fault plane attitude.

When the direction cosines (l, m, n) are expressed as functions of the fault dip (θ) and the fault strike (λ) measured from σ_y then:

$$l = \sin\theta\cos\lambda,\ m = \sin\theta\sin\lambda,\ n = \cos\theta \quad (4)$$

and equation (3) becomes:

$$\tan\omega = \cos\theta\,(\tan\lambda - 2r/\sin 2\lambda) \quad (5)$$

or rearranged in terms of the stress ratio (r):

$$r = \sin^2\lambda - \frac{\sin 2\lambda \tan\omega}{2\cos\theta}, \quad (6)$$

where

$$r = (\sigma_v - \sigma_h)/(\sigma_H - \sigma_h) \quad (7)$$

and

$$\sigma_v = \sigma_z,\ \sigma_H = \sigma_y,\ \sigma_h = \sigma_x.$$

The following sign convention is adopted: λ and θ are taken as positive and $\leq 90°$, whereas ω is taken as positive for reverse faults and as negative for normal ones.

The ratios R and r are connected through the relationships:

$$\begin{aligned} r &= R^{-1} > 1 && \text{for } \sigma_v > \sigma_H > \sigma_h \\ r &= R,\ 0 < r < 1 && \text{for } \sigma_H > \sigma_v > \sigma_h \\ r &= R/(R-1) < 0 && \text{for } \sigma_H > \sigma_h > \sigma_v. \end{aligned} \quad (8)$$

Thus, r can take any positive or negative value, whereas R varies from 0 to 1. It is pointed out that, in contrast to the ratio R, the r value alone is sufficient to describe the type of stress regime without any reference to the orientation of the principal stress axes. For example, as mentioned by Philip (1987), all three pure types of faulting, either reverse- or strike-slip or normal, have identical tensor forms characterized by the value of the intermediate stress component $\sigma_2 = (\sigma_1 + \sigma_3)/2$ and $R = 0.5$. However, the corresponding values of r are different: -1, 0.5 and 2, respectively. Moreover, since r is directly involved in equation (5), it is proposed that r should be used preferentially instead of R.

The same ratio r and equation (6) have also been applied by Simón Gómez (1986) in his y–r diagram (where y is the azimuth of σ_H), for the discrimination of the various phases of deformation in polyphase tectonics, on the basis of the striations observed on a population of reactivated fault planes. An interval of y values is delimited in which σ_H is compatible with all the fault movements. For a given fault, r is calculated for every possible direction of σ_H in the compatible field. When a tensor is responsible for the movements over a number of faults, their curves must intersect into a 'knot' defining the optimum y–r combination. Sometimes a fault population gives rise to two or more 'knots'; either several orientations of σ_H or various r ratios of the same σ_H or orientation are determined in this case.

From equation (6), for slip on a given fault with angle of sliding (ω) in the range $\omega_2 < \omega < \omega_1$, the following condition must be satisified:

$$\sin^2\lambda - \frac{\sin 2\lambda \tan\omega_1}{2\cos\theta} < r < \sin^2\lambda - \frac{\sin 2\lambda \tan\omega_2}{2\cos\theta}. \quad (9)$$

On the basis of inequality (9) a range of r values can be determined for various types of faults. For that reason the fault dip (θ) and strike (λ) need to be established.

Although it appears that the fault dip can take any value, in nature it varies within a narrow range for normal or reverse faults. Therefore, for a general discussion, the fault dip can be taken equal to the average value for each of those fault types, i.e 65° for normal faults and 25° for thrust faults. According to Sax (1946), cited by Hubbert (1951), 1650 normal faults in the Netherlands coal measures have an average dip of 63° while 450 thrust faults have an average dip of 22°.

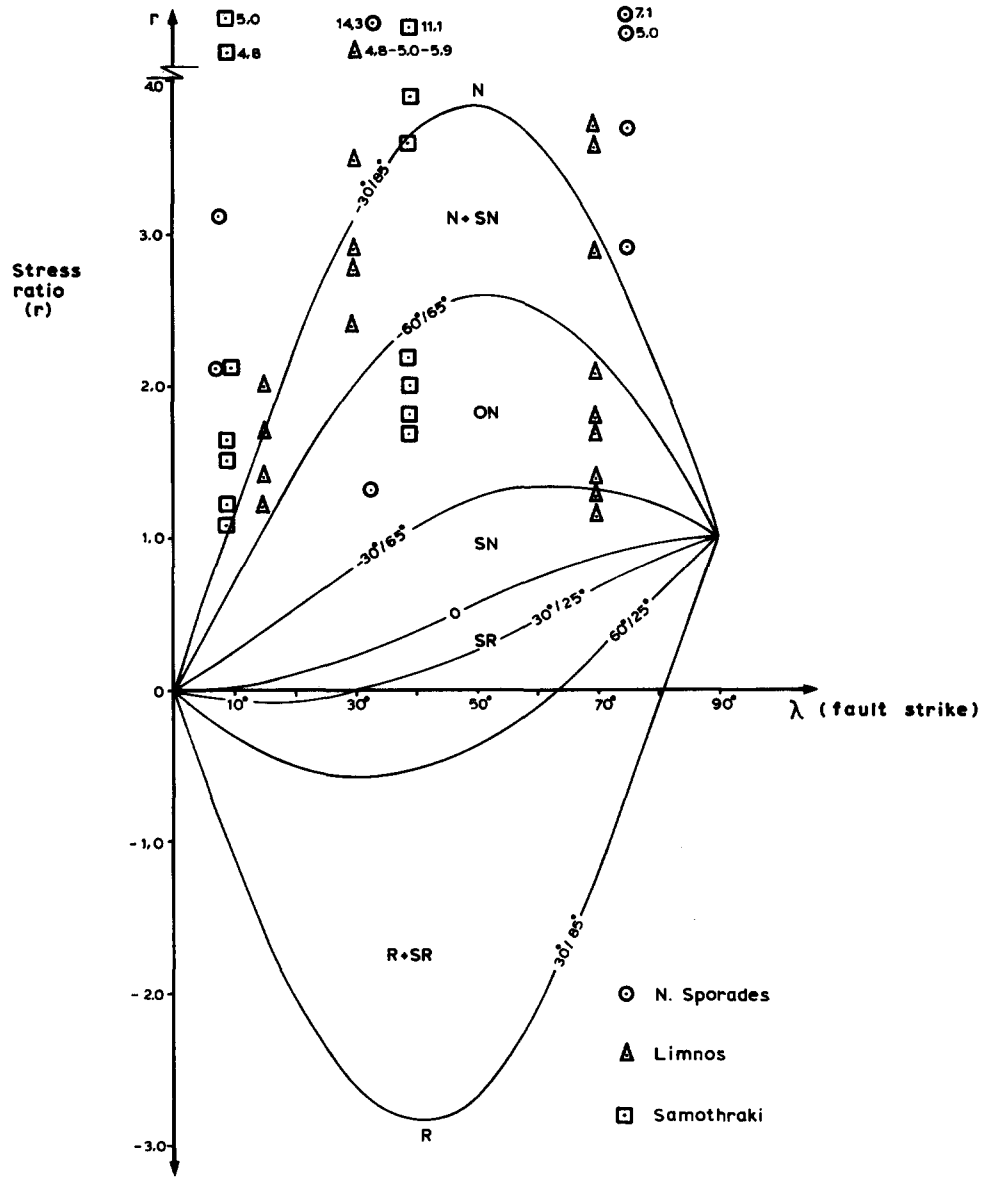

Fig. 1. Type of faulting as a function of the deviatoric stress ratio, r, and the fault strike, λ, measured from σ_H. Fault types as follows: N = normal, R = reverse, O = oblique, ON/OR = oblique with normal/reverse-slip component. Each curve corresponds to the indicated combination of angle of sliding and fault dip. Angles in degrees.

In the faulting type diagram (Fig. 1) introduced by Chiotis (1989), a number of curves are drawn by assigning certain values of ω and θ in equation (5). The angle of sliding (ω) takes the values: 0°, ±30° and ±60° which delimit the fields of strike-slip, oblique and normal or reverse types of faulting. The values 25° and 65° are assigned to the fault dip (θ) for reverse and normal faults, respectively; the dip of 85° is also considered as representative of commonly near vertical strike-slip faults. Faults of the above dips are considered as the most favourable to reactivate, under the proper stress field (Chiotis & Tsoutrelis in preparation). Areas of different types of faulting are delimited by the curves in Fig. 1 as follows:

—normal (N) for $-90° \leq \omega \leq -60°$, above the curve −60°/65°;

—oblique with normal-slip component (ON) for $-30° < \omega \leq -60°$, between the curves −60°/65° and −30°/65°;

—strike-slip with normal-slip component (SN) for $-30° \leq \omega < 0°$, between the curve −30°/65° and the zero curve for $\omega = 0°$ and any value of θ; the latter curve corresponds to the equation: $r = \sin^2 \lambda$ resulting from equation (5) for pure strike-slip faults;

—strike-slip with reverse-slip component (SR) for $0° < \omega \leq 30°$, between the zero curve and the curve 30°/25°;

—oblique with reverse-slip component (OR) for $30° < \omega \leq 60°$, between the curves 30°/25° and 60°/25°;

—reverse (R) for $60° < \omega \leq 90°$, below the curve 60°/25°;

—nearly vertical strike-slip faults with normal- or reverse-slip components between the zero curve and the curves −30°/85° and 30°/85°, respectively.

Note that a fault dip of 85° is used as representative of the approximately vertical faults, simply because an infinite value of r results from equation (6) for $\theta = 90°$, which cannot be graphically presented in Fig. 1. The infinite real interval of r $[-\infty, \infty]$ can be equivalently related to the finite interval $[-n, n]$ by plotting $r' = n -$

$[n/(r+1)]$ instead of r, as suggested by Simón Gómez (1986). This complication is considered unnecessary for our purposes.

Field data of fault dip, if available, could be used instead of the idealized values applied above. It is believed, however, that Fig. 1 can facilitate firstly the understanding of the potential co-existing fault types under various tectonic regimes and secondly the drawing out of some useful general conclusions. It is emphasized that the analysis relies on the assumption that one principal stress axis is vertical and this point will be investigated later.

The four types of tectonic deformation described by Philip (1987) are easily recognized and better defined in Fig. 1.

Type 1 (R–OR–SR), with $r \simeq 0$, corresponds to a combination of reverse faults approximately perpendicular to σ_H, along with oblique and shallow strike-slip faults.

Type 2 (N–ON–SN), $r \simeq 1$, consists of a combination of normal, oblique and strike-slip faults.

Type 3 (R–SR), a constrictive deformation with $r < -0.6$, corresponds to reverse faults of any direction and almost vertical strike-slip faults.

Type 4 (Nrd) a radial extension with $r > 2.6$, corresponds to normal and vertical strike-slip faults, both at any strike direction.

As concluded from Fig. 1, reactivation of strike-slip faults is possible for any type of stress regime, i.e. either $\sigma_v > \sigma_H > \sigma_h$, $\sigma_H > \sigma_v > \sigma_H$ or $\sigma_H > \sigma_h > \sigma_v$, i.e any value of the ratio r. This is a significant difference with the Andersonian theory of faulting, according to which strike-slip faulting occurs for $\sigma_H > \sigma_v > \sigma_h$. It is noted that, depending on the value of r, different combinations of angle of sliding and fault strike are possible for strike-slip faults. Moreover, the dip angle influences largely the area of definition of strike-slip faults, as can be seen from Fig. 1 by comparing the curves either −30°/65° and −30°/85° or 30°/25° and 30°/85°.

Among strike-slip faults, vertical or almost vertical ones are rather common. It can be shown from equation (5) that in order for a plane of weakness to act as a pure strike-slip fault ($\omega = 0°$), it must have either $\theta = 90°$ or $r = \sin^2 \lambda$. This implies that a vertical fracture of any strike can function as a pure strike-slip fault, regardless of the type of stress regime, provided that the stress field is sufficient to cause sliding. On the other hand, the alternative condition $r = \sin^2 \lambda$ requires faults of a certain strike, as well as $0 \leq r \leq 1$, which in turn implies that $\sigma_H > \sigma_v > \sigma_h$. For vertical planes with non-zero angle of sliding the stress ratio in equation (6) becomes infinite; it is concluded, therefore, that vertical discontinuities can only act as pure strike-slip faults. The special case of $\sigma_H = \sigma_h$ is not significant, even though it implies infinite r, since the shear stress vanishes then (Jaeger & Cook 1976).

It is interesting that when r varies in the range from 0 to 1, or equivalently when $\sigma_H > \sigma_v > \sigma_h$, all known types of faults are possible. Therefore, reverse faulting does not necessarily require that $\sigma_H > \sigma_h > \sigma_v$, as Anderson's model suggests; it only means that the vertical principal stress is not the greatest one.

It should also be emphasized that the deviatoric stress ratio is subjected to temporal, regional and depth-dependent variation. This was clearly demonstrated by Zoback (1989) in the actively extending northern Basin and Range province. Based on neotectonic studies, focal mechanisms, *in situ* stress measurements and other stress data, Zoback concluded that "principal stress orientations remain relatively constant with the primary variation influencing slip vectors occurring in relative stress magnitudes". Furthermore, stress field data suggest that the relative stress magnitudes measured at shallow crustal levels may not be totally representative of those at seismogenic depths.

Due to the above variation of r it is believed that Fig. 1 describes better the associated variation in the type of faulting for certain area. This is also justified by the additional reason that r ranges can be directly determined from neotectonic studies. However, the possible types of faults for specific characteristic values of r can be easier observed in Fig. 2, where the angle of sliding is plotted vs the fault strike measured from σ_H, for various combinations of r and fault dip.

APPLICATION TO THE NORTHERN AEGEAN AREA

Application to neotectonic data

The North Aegean trough is composed of subsiding geomorphological, sedimentary basins, 1000–1500 m deep, and consists of two branches (Lyberis 1984). The western one, known as Sporades basin and trending 045°, is located to the north of N. Sporades islands (Fig. 3); the eastern one, known as Saros trough, trends 075° and passes between the islands of Limnos and Samothraki. The North Aegean trough, according to Lyberis, was initiated in the Tortonian, along a fault zone at the western prolongation of the North Anatolian fault, whereas dextral strike-slip faulting is the typical mode of deformation along the North Anatolian fault zone. Distributed normal faulting and associated grabens are essential features of the North Aegean trough. A very complicated tectonic setting exists including strike-slip and reverse faulting as displayed by Roussos & Lyssimachou (1991).

There has been considerable speculation about whether the North Anatolian fault extends beneath the Aegean Sea. McKenzie (1978) suggests that it does not and motions are taken up on several structures with considerable components of normal faulting. On the other hand, Lyberis & Deschamps (1982) consider that the North Aegean trough is the active prolongation of the North Anatolian fault but the deformation there combines extension with strike-slip. In any case the tectonics of the Aegean region are significantly influenced by the westward movement of Anatolia along the North Anatolian fault (Dewey & Şengör 1979,

Şengör 1979). Since the later Serravalian (~12 Ma), the tectonics of Turkey has been dominated by the westward escape of an Anatolian block from the east Anatolian convergent zone on to the oceanic lithosphere of the Eastern Mediterranean Sea, mainly along the North and East Anatolian strike-slip faults (Şegnör *et al.* 1985).

Mercier *et al.* (1989) presented the results of a neotectonic study in the Northern Aegean islands, Thrace and Macedonia. They postulated three periods of extensional terctonics over the Northern Aegean region during: I—Middle Pleistocene–Present, with a N–S direction of estension (σ_3); II—Pliocene–early Pleistocene, with a NE direction of extension; and III—late Miocene, with a WNW direction of extension.

They also determined the azimuths of the principal stress axes and the deviatoric stress ratio $R' = (\sigma_2 - \sigma_1)/(\sigma_3 - \sigma_1)$ from the striations on a number of sites, for each of which several faults have been measured. This stress ratio R' was transformed into r through equation: $r = (1 - R')^{-1}$ valid for $\sigma_1 = \sigma_v$, which is the case for the data used. The results for the nearest islands to the North Aegean trough are shown in Table 1.

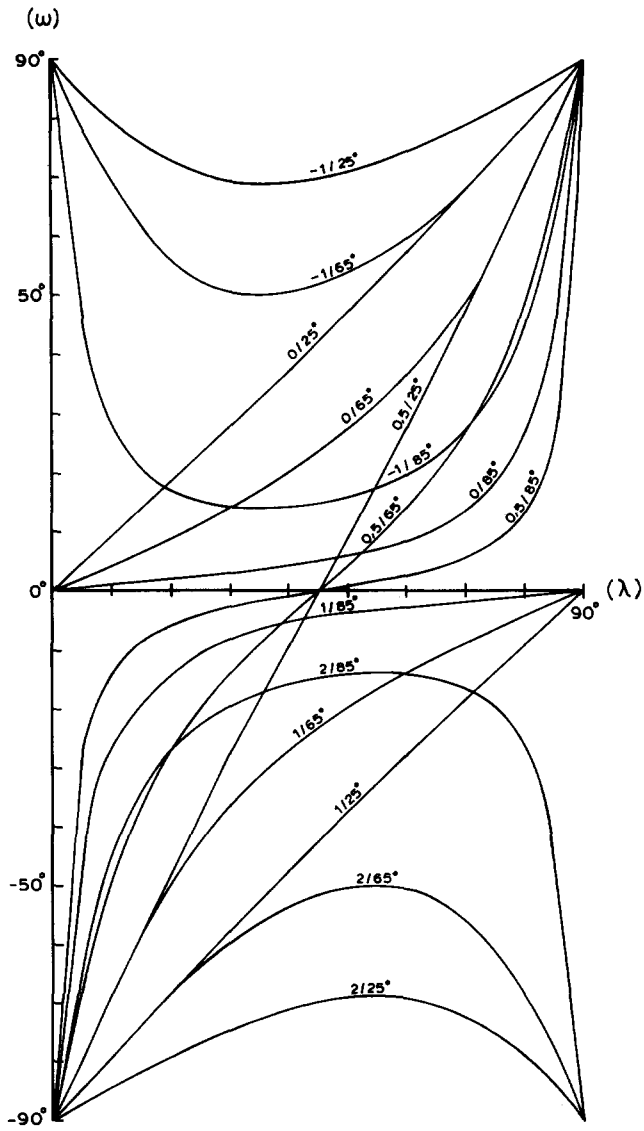

Fig. 2. Angle of sliding, ω, vs the fault strike, λ, measured from σ_H for various combinations of deviatoric stress ratio r/fault dip. Angles in degrees.

Before applying the Fault-type diagram to the neotectonic data of the Northern Aegean we should check whether the basic assumption holds that one of the principal stress axes is almost vertical. Two sources of information were used: the azimuths of principal stress axes as determined by Mercier *et al.* (1989); and the azimuths of the P and T axes for the most reliable focal mechanisms of shallow earthquakes in the Aegean and the surrounding areas, compiled by Papazachos & Papazachou (1989). As shown in Fig. 4(a), one of the principal stress axes determined from neotectonic data is maintained almost vertical (>60°), which does not always hold for the axes P, B and T (Fig. 4c).

This suggests that at the relatively shallow depths corresponding to the neotectonic observation one of the principal stress axes is retained vertical. There is in general a lack of direct information on the orientation of the stress field axes at the earthquake foci due to the fact that the P and T axes determined from the focal mechanisms are not usually related to the regional stress field in any simple manner (McKenzie 1972).

The calculated values of stress ratio r for the islands of N. Sporades, Limnos and Samothraki which surround the North Aegean trough are shown in Table 1 and plotted in the Fault-type diagram (Fig. 1). The fault strike plotted refers to the main fault forming the southern border of the trough; the angle of fault strike with σ_H is also shown in Table 2. From the distribution of the points in Fig. 1, it is concluded that three types of neotectonic faulting are possible in the North Aegean basins from late Miocene to present, as follows:

(a) for high values of r ($r > 2.6$), radial extension with normal faulting in all possible directions in conjunction with strike-slip faulting on almost vertical faults of any direction;

(b) for intermediate values of r ($1.5 < r < 2.5$) a combination of normal, oblique normal faults with strike-slip faults of high dip (>60°). Fault orientation tends to follow roughly some preferred possible strikes such as subparallel or approximately perpendicular to σ_H for normal and almost vertical strike-slip faults, intermediate between the above end-cases for oblique faults and around 45° to σ_H for strike-slip faults dipping about 70°;

(c) for $r \simeq 1$, a combination of normal, oblique and strike-slip faults, where normal faults are subparallel to σ_H, oblique faults at angles 45° to σ_H and strike-slip faults can have any dip or direction.

The described application of Fig. 1 is useful for the assessment of the expected type of faulting in a certain area. However, for the estimation of the sense of movement along a particular fault plane the most appropriate approach is the calculation of the angle of sliding ω through equation (5). This may be illustrated for the fault bordering the southern margin of the North Aegean trough.

The data used (Table 2) are the deviatoric stress ratio and the azimuth of σ_H derived both from the neotectonic

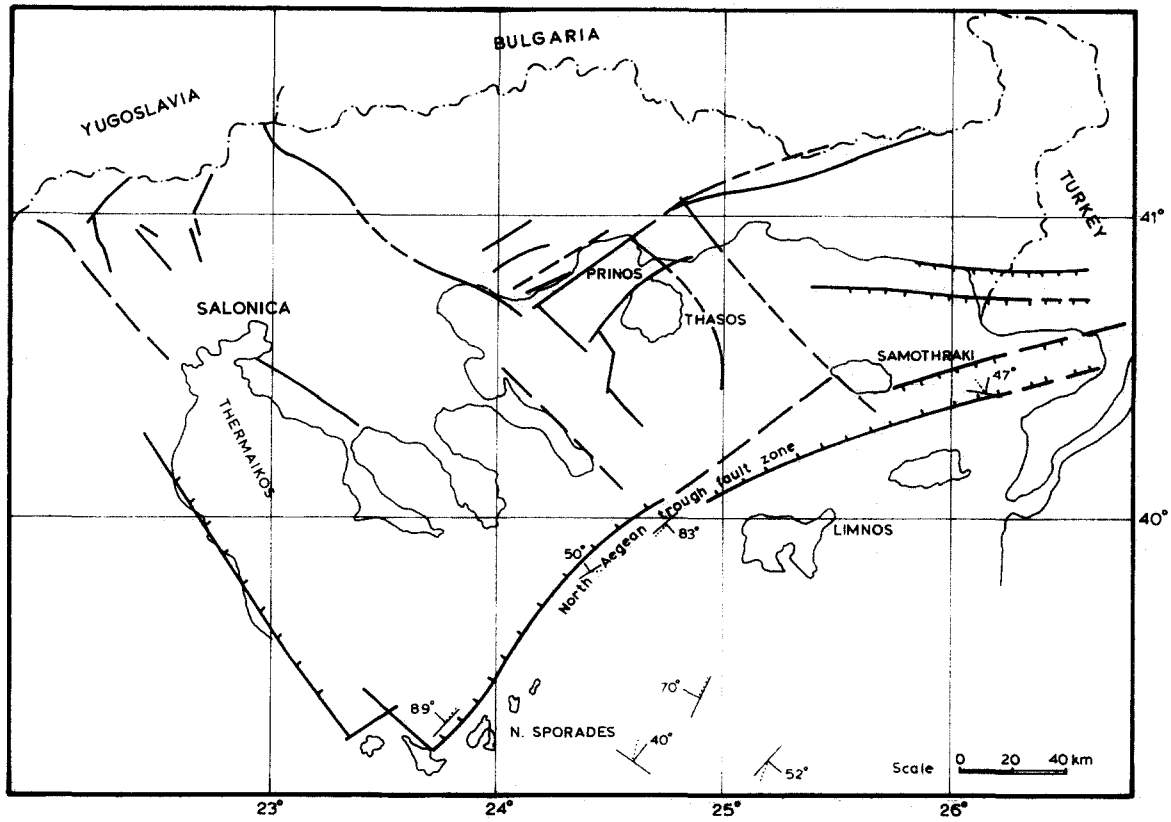

Fig. 3. Structural sketch of the areas surrounding the North Aegean trough fault zone after Mercier *et al.* (1989). Assumed fault planes from earthquake mechanisms are also shown; fault attitude and direction of sliding (dotted) are graphically depicted; fault dip is also given numerically.

study by Mercier *et al.* (1989), and the fault strike and dip estimated from marine seismic sections.

A deep seismic profile northwest of Limnos (Lalechos & Savoyat 1979, fig 8) shows that the southernmost fault bordering the eastern branch of the North Aegean trough dipped ~85°NW during the deposition of the Miocene, Plio-Pleistocene and present sediments. In contrast, the fault dip in the western branch was not constant during the same period. It dips presently at ~85°NW, as shown in a sparker record published by Brooks & Ferrentinos (1980, fig. 6). However, during the Miocene, the Sporades basin was bordered by a subparallel normal fault dipping approximately 45°NW, based on results from another seismic section of Lalechos & Savoyat (1979, fig. 7). Subsidence during the Pliocene took place along another parallel fault of the same dip. Certain significant conclusions can be drawn from Table 2.

First, a rather broad range of stress ratio is found during periods of constant orientation of the stress field, which implies a fluctuation of the relative magnitude of the involved tectonic stresses. This fluctuation can cause extreme variations in the type of faulting, such as from normal to strike-slip faulting in N. Sporades during period I, as well as in Limnos during period II and in Samothraki during periods I and II. Such an effect

Table 1. Deduced types of faulting on the basis of the r ratio (in brackets) determined from neotectonic studies by Mercier *et al.* (1989) for the areas surrounding the North Aegean trough during: (i) Middle Pleistocene to Present (period I); (ii) Pliocene to early Pleistocene (II); and (iii) late Miocene (III). Nrd = radial extension; the rest types of faulting are symbolized as in Fig. 1

	$r = (\sigma_v - \sigma_h)/(\sigma_H - \sigma_h)$		
Area	Period I	Period II	Period III
N. Sporades	Nrd/N–ON–SN (1.3, 14.3)	Nrd (2.9, 3.7, 5.0, 7.1)	Nrd/N–ON (2.1, 3.1)
Limnos	N–ON–SN (1.2, 1.4, 2 × 1.7, 2.0)	N–ON–SN/Nrd (1.2, 1.3, 1.4, 1.7, 1.8, 2.1, 2.9, 2 × 3.6, 3.7)	Nrd (2.4, 2.8, 2 × 2.9, 3.5, 4.8, 5.0, 5.9)
Thassos	Nrd/N–ON (1.9, 3.5, 11.1)	Nrd (1.5, 3.2, 4.8, 7.1, 3 × 8.3)	Nrd/N–ON (1.6, 2.3, 2.4, 2.6)
Samothraki	Nrd/N–ON–SN (1.1, 1.2, 1.5, 2 × 1.6, 2.1, 4.8, 5.0)	Nrd/N–ON (1.7, 2.2, 3.6, 11.1)	Nrd/N–ON (1.8, 2.0, 3.9)

cannot be produced from fluctuations of the intensity of extensional tectonics, assuming that extension is the only tectonic mechanism. It requires, therefore, the interplay between extensional and compressional tectonics, the latter resulting in an increase of σ_H and a decrease of the deviatoric stress ratio r. Obviously, this compression is associated with the westward movement of Anatolia, which is therefore postulated to be episodic.

Second, the main faults bordering the eastern branch of the North Aegean trough behaved predominantly as strike-slip faults with intervals of oblique or normal faulting.

Third, it is inferred that the compressive influence of Anatolia has propagated westwards gradually since the late Miocene. Indeed, strike-slip faulting is inferred in Samothraki since period III, in Limnos since period II and in N. Sporades only since period I.

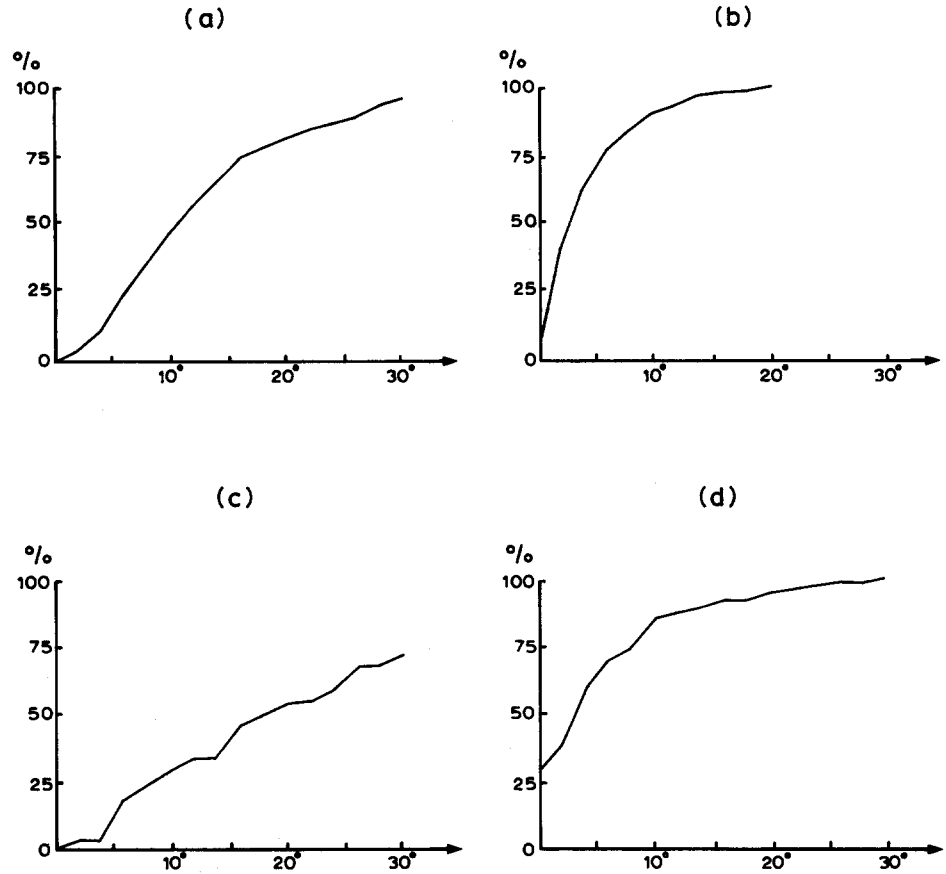

Fig. 4. (a) Cumulative relative frequency of the least deviation from the vertical for the principal stress axes in the Northern Aegean, based on 108 neotectonic determinations by Mercier *et al.* (1989). (b) As above, for the least deviation from the horizontal. (c) Cumulative relative frequency of the least deviation from the vertical for 55 determinations of the *P*, *B* and *T* axes from the most reliable focal mechanisms in Greece, as compiled by Papazachos & Papazachou (1989). (d) As in (c), for the least deviation from the horizontal.

Table 2. Calculated angle of slip along the fault zone bordering southwards the North Aegean trough. Angles in degrees; periods as in Table 1

Area—Period	Deviatoric stress ratio r	Mean azimuth of σ_H	Azimuth of fault strike	Angle λ	Fault dip	Calculated angle of sliding
N. Sporades—I	1.3, 14.3	68	35	33	85	−11, −70
N. Sporades—II	2.9, 3.7, 5.0, 7.1	140	35	75	45	−80, −83, −85, −87
N. Sporades—III	2.1, 3.1	28	35	7	45	−85, −87
Limnos—I	1.2, 1.4, 2 × 1.7, 2.0	85	70	15	85	−22, −25, 2 × (−30), −34
Limnos—II	1.2, 1.3, 1.4, 1.7, 1.8, 2.1, 2.9, 2 × 3.6, 3.7	140	70	70	85	−14, −19, −23, −33, −36, −44, −58, 2 × (−65), −66
Limnos—III	2.4, 2.8, 2 × 2.9, 3.5, 4.8, 5.0, 5.9	40	70	30	85	−52, −57, 2 × (−58), −63, −70, −71, −74
Samothraki—I	1.1, 1.2, 1.5, 2 × 1.6, 2.1, 4.8, 5.0	79	70	9	85	−31, −34, −40, 2 × (−42), −50, 2 × (−70)
Samothraki—II	1.7, 2.2, 3.6, 11.1	134	70	64	85	−10, −17, −32, −66
Samothraki—III	1.8, 2.0, 3.9	31	70	39	85	−14, −16, −32

Application to earthquake focal mechanisms

The solutions of the earthquake focal mechanisms can also be used for the estimation of the deviatoric stress ratio from equation (5).

This is attempted here for the North Aegean trough based on the data of Table 3 derived from Papazachos & Papazachou (1989). Two alternative values of the stress ratio, r_1 and r_2, were calculated one for each nodal plane N_1 and N_2, respectively. Taking into account the general tectonic setting and the alternative ratios r_1 and r_2, the fault plane was selected as indicated in the Table 3.

It was assumed that one of the principal stress axes is vertical based on the neotectonic stress field data and the fact that out of the eight focal mechanisms of Table 3, five of them have one of the P, B, T axes close to vertical and the other three result in compatible r values. Furthermore, the azimuth of σ_H was taken equal to the mean horizontal projection of the T axes, determined from the focal mechanisms, which is 88°. The stress ratios calculated from the focal mechanisms shown in Table 3 suggest that any type of faulting can be expected in the North Aegean trough, because r varies within a broad range including values less than 1 or even negative.

This confirms the conclusion of Papazachos *et al.* (1984) that the northern Aegean and the northwestern-most part of Anatolia is a zone of dextral faulting accompanied by thrust or normal component and that the ridge- or trench-like nature of the Northern Aegean trough may not be resolved.

If the first two earthquakes of Table 3 are omitted due to their largely deviating values of r, an average value of 0.5 is calculated for the rest. If this value of r is considered representative of the North Aegean trough, the possible types of faulting are approximately those enclosed by the curves 0.5/25° and 0.5/85° of Fig. 2. Therefore, normal faulting would be expected parallel to σ_H, reverse perpendicular to σ_H, strike-slip for any intermediate fault orientation, oblique with normal component for strikes at angles <30° with σ_H and oblique faulting with reverse-slip component at angles >60° with σ_H.

It must be emphasized that due to the episodic character of the compressional tectonics in the trough, conclusions from seismological data cannot be generalized over the period from the late Miocene to present. However, the neotectonic evidence of extension in the Northern Aegean (Mercier *et al.* 1989) is compatible with the seismological indications of compression and the same planes are reactivated either as normal or as strike-slip faults depending on the value of r, which varies periodically.

CALCULATION OF r FOR ROTATED STRESS FIELD

In the case that none of the principal stress axes is approximately vertical, additional data are required for the calculation of the deviatoric stress ratio r, defined now as $r = (\sigma_z - \sigma_x)/(\sigma_y - \sigma_x)$ from equation (3). The procedure is simple in the common case when the principal stress axes σ_x and σ_z are rotated around the third axis σ_y at an angle ϕ. Equation (3) can again be used, provided that the direction cosines and angle of sliding are referred to the rotated principal stress axes. If θ is the dip of the fault and λ is its strike measured from σ_y, then the direction cosines l', m', n' of the normal to the fault plane relative to the rotated principal stress axes are modified due to the rotation as follows:

$$\begin{aligned} l' &= l\cos\phi + n\sin\phi \\ m' &= m \\ n' &= -l\sin\phi + n\cos\phi, \end{aligned} \tag{10}$$

where l, m, n are direction cosines referred to the original co-ordinate system before the rotation, given by the equation (4). Thus the direction cosines to be used in equation (3) are:

$$\begin{aligned} l' &= \sin\theta\cos\lambda\cos\phi + \cos\theta\sin\phi \\ m' &= \sin\theta\sin\lambda \\ n' &= -\sin\theta\cos\lambda\sin\phi + \cos\theta\cos\phi. \end{aligned} \tag{11}$$

From numerical application of the above formulae it can be seen that for $\phi > 45°$ and $\theta < 25°$, which is the case in North Aegean, the effect of the axes rotation is not significant for the estimation of the direction of sliding and can be ignored in first approximation.

Table 3. Focal mechanisms for the earthquakes in the North Aegean trough compiled by Papazachos & Papazachou (1989). For the pressure (P) and tension (T) axes λ and θ are their pitch and plunge, respectively. For the nodal planes (N_1 and N_2) λ, θ and ω correspond to the strike, the dip and the angle of slip. The deviatoric ratios r_1 and r_2 correspond to the two nodal planes. The selected fault plane and the respective stress ratio are shown in the last two columns. Angles in degrees; M = magnitude

	Co-ordinates			P		T		N_1			N_2						
Date	φ° N	λ° E	M	λ	θ	λ	θ	λ	θ	ω	λ	θ	ω	r_1	r_2	Fault plane	r
9 Mar. 1965	39.3	23.8	6.1	266	04	174	04	220	89	173	310	86	01	−3.0	0.3	N_1	−3.0
4 Mar. 1967	39.2	24.6	6.6	314	75	200	06	98	54	−107	304	40	−68	−0.9	1.9	N_2	1.9
19 Feb. 1968	39.4	24.9	7.1	68	11	160	15	205	70	179	294	89	20	0.8	−8.0	N_1	0.8
27 Mar. 1975	40.4	26.1	6.6	259	47	157	07	41	60	128	279	47	−44	1.8	0.3	N_2	0.3
19 Dec. 1981	39.2	25.2	7.2	255	35	357	16	42	52	−165	302	78	−39	0.7	2.1	N_1	0.7
27 Dec. 1981	38.8	24.9	6.5	77	05	168	02	213	86	−177	122	87	−4	1.1	0.9	N_1	1.1
18 Jan. 1982	39.8	24.4	7.0	106	10	207	47	235	50	153	343	70	43	−0.1	0.2	N_1	−0.1
6 Aug. 1983	40.0	24.7	7.0	272	04	02	05	48	83	178	138	88	07	0.3	−1.2	N_1	0.3

CONCLUSIONS

The angle of slip on pre-existing faults largely depends on the deviatoric stress ratio, r, the effect of which on the type of faulting can in general be studied through a diagram of the form of Fig. 1, drawn on the assumption that one of the principal stress axes is approximately vertical. The four types of tectonic deformation according to Philip (1987) can easily be recognized in this diagram. The diagram also facilitates understanding of the potential co-existance of different fault types under various tectonic regimes. It is inferred from Fig. 1 that when $0 \leq r \leq 1$, or equivalently $\sigma_h \leq \sigma_v \leq \sigma_H$, all known types of faults are possible. Therefore, reverse faulting does not necessarily require that $\sigma_v < \sigma_h < \sigma_H$. Similarly strike-slip faulting is possible for any value of the deviatoric stress ratio and is the only possible type of faulting on vertical faults.

Based on regional geological evidence it is postulated that tectonic strain at the higher structural level is accommodated along pre-existing major crustal fault zones. The North Aegean trough is treated as an example of this type of deformation. Azimuths of the principal stress axes determined in Northern Aegean by Mercier *et al.* (1989) suggest that one of the principal stress axes has been approximately vertical since the late Miocene. Three periods of constant stress field orientation but with a wide range of the stress ratio, r, are calculated from neotectonic data on the islands bordering the North Aegeran trough. The variation in r is interpreted as a result of episodic increase of σ_H associated with the westward movement of Anatolia along the North Anatolian fault, superimposed on a continuing extension. This compressive influence gradually increased in each area of the trough, since the late Miocene, and propagated gradually westwards.

Stress ratios calculated from earthquake focal mechanisms suggest a current period of compression from Anatolia. Combined with neotectonic evidence of extension all over the Northern Aegean, it is postulated that episodes of tectonic compression overlap due to the westwards movement of Anatolia along the North Anatolian fault.

Acknowledgements—Our initial manuscript was substantially improved thanks to the constructive comments and suggestions by D. J. Sanderson and two anonymous referees. We are grateful to all of them.

REFERENCES

Anderson, E. M. 1951. *The Dynamics of Faulting*. Oliver & Boyd, Edinburgh.

Angelier, J. 1979. Determination of the main principal directions of stresses for a given fault population. *Tectonophysics* **56**, T17–T26.

Arthaud, F. 1969. Méthode de détermination graphique des directions de raccourcissement, d'allongement et intermédiaire d'une population de failles. *Bull. Soc. geol. Fr.* **7**, 729–737.

Bott, M. H. P. 1959. The mechanics of oblique slip faulting. *Geol. Mag.* **96**, 109–117.

Brace, W. F. & Kohlstedt, D. L. 1980. Limits on lithospheric stress imposed by laboratory experiments. *J. geophys. Res.* **85**, 6248–6252.

Brooks, M. & Ferentinos, G. 1980. Structure and evolution of the Sporades basin of the North Aegean trough, Northern Aegean Sea. *Tectonophysics* **68**, 15–30.

Carey, E. 1976. Analyse numerique d'un Modele mechanique elementaire appliqué a l'Etude d'une Population de Failles: Calcul d'un Tenseur moyen des contraintes a partir des Stries des Glissement. Unpublished thèse 3e cycle, Tectonique generale, Paris-Sud.

Chiotis E. 1989. Thermomechanical behaviour of the lithosphere in Greece. Unpublished Ph.D. thesis, National Technical University, Athens.

Dewey, J. F. & Şengör, A. M. C. 1979. Aegean and surrounding regions: complex multiplate and continuum tectonics in a convergent zone. *Bull. geol. Soc. Am.* **90**, 84–92.

Hubbert, M. K. 1951. Mechanical basis of certain familiar geological structures. *Bull. geol. Soc. Am.* **62**, 355–371.

Jaeger, J. C. & Cook, N. G. W. 1976. *Fundamentals of Rock Mechanics*. Chapman & Hall, London.

Lalechos, N. & Savoyat, E. 1979. La sédimentation néogene dans le fossé Nord Egeen. *VI Colloquium on the Geology of the Aegean Region*, Athens, **2**, 591–603.

Lyberis, N. 1984. Tectonic evolution of the North Aegean trough. In: *The Geological Evolution of the Eastern Mediterranean* (edited by Dixon, J. E. & Robertson, A. H. F.) *Spec. Publs geol. Soc. Lond.* **17**, 709–725.

Lyberis, N. & Deschamps, A. 1982. Sismo-tectonique du fossé Nord-Egeen: relations avec la faille Nord-Anatolienne. *C. r. Acad. Sci, Paris* **295**, 625–628.

McKenzie, D. 1972. Active tectonics of the Mediterranean region. *Geophys. J. R. astr. Soc.* **30**, 109–185.

McKenzie, D. 1978. Active tectonics of the Alpine–Himalayan belt: the Aegean Sea and surrounding regions. *Geophys. J. R. astr. Soc.* **55**, 217–245.

Mercier, J. L., Sorel, D., Vergely, P. & Simeakis, K. 1989. Extensional tectonic regimes in the Aegean basins during the Cenozoic. *Basin Res.* **3**, 49–71.

Papazachos, B. C., Kiratzi, A. A., Hatzidimitriou, P. M. & Rocca, A. C. 1984. Seismic faults in the Aegean Sea. *Tectonophysics* **106**, 71–85.

Papazachos, B. & Papazachou, K. 1989. *The Earthquakes of Greece* (in Greek). Ziti, Thessaloniki.

Philip, H. 1987. Plio-Quaternary evolution of the stress field in Mediterranean zones of subduction and collision. *Annales Geophysicae* **5B**, 301–319.

Reches, Z. 1983. Faulting of rocks in three-dimensional strain fields. II. Theoretical analysis. *Tectonophysics* **95**, 133–156.

Rousos, N. & Lyssimachou, T. 1991. Structure of the Central North Aegean trough: an active strike-slip deformation zone. *Basin Res.* **3**, 39–48.

Sax, H. G. J. 1946. De tectonick van het Carboon in het Zuid-Limburgsche mijngebieb. *Meded. geol. Stricht.*, Ser. C-I-I, No. 3.

Şengör, A. M. C. 1979. The North Anatolian transform fault: its age, offset and tectonic significance. *J. geol. Soc. Lond.* **136**, 269–282.

Şengör, A. M. C., Gorur, N. & Saroglu, G. 1985. Strike-slip faulting and related basin formation in zones of tectonic escape: Turkey as a case study. In: *Strike-slip Deformation, Basin Formation and Sedimentation* (edited by Biddle, K. T. & Christie-Blick, N.). *Spec. Publs Soc. econ. Palaeont. Miner.* **37**, 227–264.

Sibson, R. H. 1985. A note on fault reactivation. *J. Struct. Geol.* **7**, 751–754.

Simón Gómez, T. L. 1986. Analysis of a gradual change in stress regime (example from the eastern Iberian chain, Spain). *Tectonophysics* **124**, 37–53.

Zoback, M. L. 1989. State of stress and modern deformation of the Northern Basin and Range province. *J. geophys. Res.* **94**, 7105–7128.